JOURNAL OF APPLIED ELECTROCHEMISTRY 9 (1979) 545–554

Anodic electrochemistry of chalcopyrite

T. BIEGLER, D. A. SWIFT

CSIRO Division of Mineral Chemistry, PO Box 124, Port Melbourne, Victoria 3207, Australia

Received 24 July 1978

The anodic behaviour of chalcopyrite in 1 M H_2SO_4 and 1 M HCl was studied by linear sweep voltammetry and potentiostatic electrolysis. Voltammograms with a fresh surface showed a small prewave, attributed to a surface oxidation process, followed by a region of active dissolution characterized by a steeply rising anodic current. At still higher potentials the behaviour differed in the two electrolytes, but, contrary to a previous report, there was no evidence of a photosensitive limiting current. Anodic characteristics of chalcopyrite specimens from different sources, including synthetic material, were similar. The anode reaction was found to involve 6·7 ± 0·3 F per mole of chalcopyrite, from which it was calculated that 86% of the sulphide sulphur was oxidized to the elemental form (some of which was plastic sulphur) and 14% to sulphate. The surfaces of oxidized electrodes were examined and photographed after varying periods of potentiostatic electrolysis. Chalcopyrite dissolution occurred at localized sites, the number of which depended strongly on potential. Current–voltage and potentiostatic current–time curves were interpreted in terms of the kinetics of nucleation, growth and overlap of these discrete corrosion centres.

1. Introduction

The present investigation of the anodic behaviour of chalcopyrite ($CuFeS_2$) was aimed at an improved understanding of processes in which copper is leached from this mineral under oxidizing conditions in acidic aqueous solutions. Such processes occur, for example, in the leaching of copper waste dumps and in a variety of hydrometallurgical processes which have been proposed for the treatment of copper concentrates (see e.g. [1]). The principle underlying this type of study is that, in general, the dissolution of semiconducting sulphide minerals in oxidizing solutions is an electrochemical corrosion process in which a soluble oxidant such as ferric ion or oxygen is reduced at the mineral surface, which itself behaves as an anode. Electrochemical studies might therefore hope to establish the mechanism and rate-determining steps of the anode and cathode reactions involved, the overall rate-controlling process, the potential-dependence of the reaction mechanisms and product compositions, and possible roles played by semiconducting properties and mineral origin.

Several reports of the anodic behaviour of chalcopyrite are available [2–6], but the different aims and conditions employed in the experiments make comparisons difficult. All show anodic polarization curves with a region where current depends steeply on potential, sometimes with several steps or inflections [5, 6], and an approach to a limiting current at high potentials. The anodic reaction was stated [3] to be

$$CuFeS_2 \rightarrow Cu^{2+} + Fe^{2+} + 2S + 4e \qquad (1)$$

but others [5, 6] report that the stoichiometry corresponds to a combination of

$$CuFeS_2 \rightarrow Cu^{2+} + Fe^{3+} + 2S + 5e \qquad (2)$$

and

$$CuFeS_2 + 8H_2O \rightarrow Cu^{2+} + Fe^{3+} + 2SO_4^{2-} + 16H^+ + 17e\,. \qquad (3)$$

These discrepancies will be discussed below.

It has been claimed [3, 4] that illumination affects the anodic behaviour of chalcopyrite, and it was concluded [3, 4] that the transport of minority carriers within the electrode becomes rate-limiting at high anodic currents. On the other hand, Springer [2] could find no evidence that the semiconducting properties of chalcopyrite influenced its electrochemical behaviour. The question is re-examined here.

0021–891X/79/050545–10 $03·00/0

2. Experimental

Electrochemical experiments were carried out at constant or programmed (linear sweep) potentials with conventional instrumentation. In general, rotating electrodes (50 rev s^{-1} was usually chosen) were used in potential sweep measurements and stationary electrodes in longer-term constant potential runs. Electrodes were prepared from high quality natural specimens of massive chalcopyrite showing no foreign inclusions under the microscope, and one sample of synthetic material (kindly supplied by Dr. J. E. Dutrizac of CANMET). The natural chalcopyrite came from Moonta (South Australia), Mt. Lyell (Tasmania) and Ookiep (South Africa), with one sample of unknown origin. Methods used for preparing stationary and rotating electrodes (for use with a Beckman variable speed rotator) have been outlined in recent publications [7, 8]. Preparation of electrode surfaces after coarse grinding was completed either on 600 grade silicon carbide paper (designated as a ground surface) or by further polishing with 0·3 μm alumina (polished surface).

The glass electrolysis cells had three compartments with a sintered disc separating working and counter electrodes and a Luggin probe for the reference electrode compartment. A saturated calomel reference electrode, whose potential was taken as 0·245 V versus standard hydrogen electrode (SHE), was employed. All potentials are referred to the SHE. Oxygen was purged from the solutions with a nitrogen stream. All measurements were carried out at 25° C.

3. Results and discussion

3.1. *Current–voltage behaviour*

The curve in Fig. 1, drawn on a logarithmic scale to show features over a wide range of currents, is representative of the first scan with a freshly ground surface in 1 M H_2SO_4. Comparisons with the behaviour in 1 M HCl are given later.

Three regions can be defined. From the rest potential (around 0·4 V versus SHE) to 0·85 V (polished) or 0·95 V (ground) there was a broad prewave in which the current passed through a peak or a plateau, depending on the conditions used. If the electrode potential was cycled, this

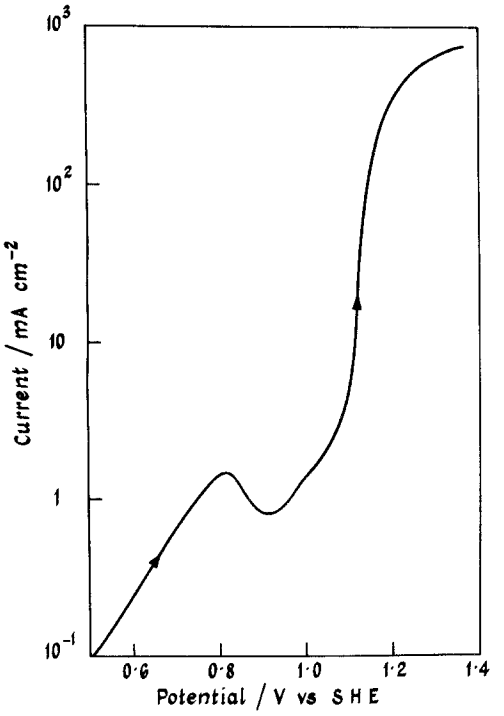

Fig. 1. Current–voltage curve on first positive-going sweep with a ground chalcopyrite surface in 1 M H_2SO_4 (sweep rate 20 mV s^{-1}; rotation rate 50 rev s^{-1}).

prewave was absent from the second and subsequent scans. Between 0·95 V and 1·2 V the current passed through the range 1–100 mA cm^{-2} and, although the logarithmic plot has no substantial linear segment, the steepest portion corresponds to a Tafel slope of around 30 mV. Beyond 1·2 V

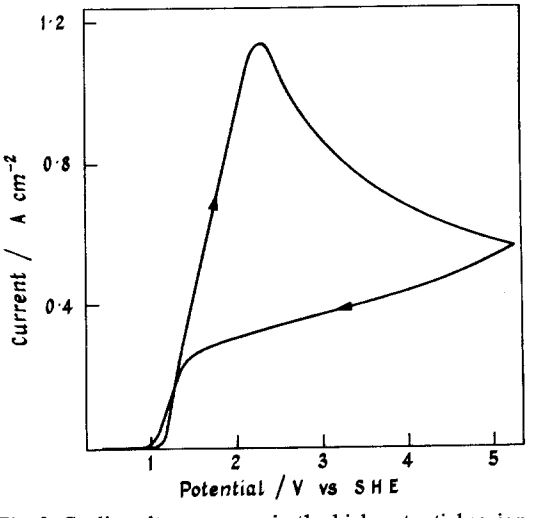

Fig. 2. Cyclic voltammogram in the high potential region (1 M H_2SO_4; sweep rate 200 mV s^{-1}; rotation rate 50 rev s^{-1}).

the current–voltage relationship (Fig. 2) was linear before reaching a peak at an apparent potential of 1·8–3·5 V, depending on the specimen and the sweep rate. The reverse scan showed considerable hysteresis.

3.2. *Prewave*

The prewave was present in both electrolytes used but was studied systematically only in 1 M H_2SO_4. As mentioned above, it appeared on the first sweep with a freshly prepared surface (Fig. 3). Delays of more than about 1 min between surface preparation and commencement of the sweep tended to decrease the definition of the prewave and the charge passed in the prewave region.

The prewave charge was determined by integration to either the minimum in the current or the inflection in the curve immediately below the main wave (see Fig. 3). The procedure is arbitrary but seems appropriate in view of the incomplete separation of the prewave and the different curve shapes found under different conditions. The results in Table 1 show only a small variation in prewave charge with sweep rate. Similarly, there was only a small dependence on rotation rate, a 12% decrease between zero and 100 rev s^{-1} (sweep rate 20 mV s^{-1}). Prewaves for polished and ground surfaces differed in shape (Fig. 3) and charge. For a ground surface the charge was 16 mC cm^{-2} (at 20 mV s^{-1}), i.e. about 11 times the value for a polished surface.

Our interpretation of these results is that the prewave represents a surface oxidation process involving a thin layer of chalcopyrite. The charge passed in completing this process is of the order of 1 mC per real cm^2 (actual charges are higher because of surface roughness), which corresponds to a chalcopyrite layer $4{\cdot}6/n$ nm thick, where n is the number of Faradays per mole of chalcopyrite in the prewave reaction. Identification of this reaction has important practical implications since the potential range of the prewave covers the potentials expected in the ferric leaching of copper ores (E^0 for Fe^{3+}/Fe^{2+} is 0·77 V). However, the very small thickness of the product layer would seem to preclude its direct identification by conventional techniques such as X-ray diffraction. In an attempt to grow a thicker layer, a polished chalcopyrite electrode was held potentiostatically within the prewave range or slightly beyond (up to 0·95 V) for periods of up to an hour, at which stage the current had fallen to around 0·1 μA cm^{-2}. The electrode still retained the appearance of

Table 1. Prewave charge as a function of sweep rate for polished chalcopyrite (1 M H_2SO_4; 50 rev s^{-1})

Sweep rate (mV s^{-1})	*Prewave charge* (mC cm^{-2})
4	1·25
10	1·38
20	1·50
40	1·14
100	1·14

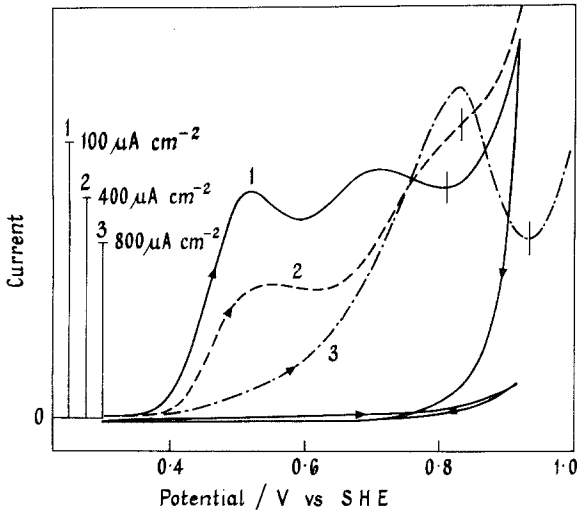

Fig. 3. First linear sweep voltammograms with freshly prepared surfaces (1 M H_2SO_4; rotation rate 50 rev s^{-1}). Curve 1: polished, 20 mV s^{-1}; curve 2: polished, 100 mV s^{-1}; curve 3: ground, 20 mV s^{-1}. Return sweep and second cycle shown for curve 1 only. Integration limits marked by vertical line.

polished chalcopyrite and the X-ray analysis showed no other material present.

The results of ferric leaching studies on particulate chalcopyrite [9, 10] lead us to believe that even longer term experiments would fail to build up a significantly thicker layer of 'prewave product'. Linge [9] found a dissolution rate after 1 hour equivalent to an anodic current of only 0·02 $\mu A\ cm^{-2}$ (i.e. consistent with our electrochemical measurements), while in the long term elemental sulphur was formed. From analysis of dissolved copper and iron, he postulated that a layer of metal-deficient lattice formed at first, building up rapidly to a limiting thickness of about 5 nm. Further reaction led to sulphur, according to Equation 2. It seems reasonable to equate this initial leaching stage with the prewave process observed here. The implication of this conclusion is that potentiostatic oxidation of chalcopyrite below about 0·95 V would also ultimately produce sulphur, though very long periods would be required to yield an identifiable layer, e.g. at 0·1 $\mu A\ cm^{-2}$ a sulphur thickness of 1 μm would take 180 days to form according to Reaction 2.

Both Linge [9] and Baur *et al.* [10] have shown that the initial leaching stage involves selective dissolution of iron. The shorter the time of measurement, the higher is the Fe/Cu ratio obtained, e.g. Baur *et al.* [10] found a ratio of 6·6 at 30 s, while Linge [9] reported a ratio of about 2 over the first 5 min. As the former time scale is more appropriate to our sweep measurements we conclude that the prewave process involves the initial dissolution of metal from the sulphide lattice, with substantially more iron dissolving than copper.

3.3. *The anode reaction*

The process in the main wave region (potential 1 V and above) will now be considered. Dissolved copper and iron were determined in potentiostatic experiments in which the charge passed was in the range 30–150 C over periods of 6 min to 31 h. Within experimental error (± 2%), equimolar quantities of the two metals were found. In some 20 determinations over the potential range examined (1·0–1·2 V in both 1 M H_2SO_4 and 1 M HCl), the charge passed was 6·7 ± 0·3 F per mole of dissolved iron or copper.

This figure allows quantitative assessment of the contributions from different reaction pathways. To start with, we exclude Reaction 1 since, independent of its ionic state in the chalcopyrite lattice (which in [3] was regarded as a significant factor), iron must enter solution in the ferric state at the potentials under consideration. Reactions 2 and 3 differ in the degree of oxidation of the sulphur. If x is the fraction of chalcopyrite oxidized according to Reaction 3, the composite equation representing the total process is

$$CuFeS_2 + 8xH_2O \rightarrow Cu^{2+} + Fe^{3+} + 2xSO_4^{2-} + 2(1-x)S + 16xH^+ + (12x+5)e. \quad (4)$$

With the above data, $(12x + 5) = 6{\cdot}7 \pm 0{\cdot}3$ and $x = 0{\cdot}141 \pm 0{\cdot}025$, i.e. about 14% of the chalcopyrite is oxidized to sulphate and 86% to sulphur. From analogous experiments over a wide potential range, Bertram and Illi [5] obtained a current efficiency of 76% for copper dissolution according to Reaction 2. Calculated this way, our data give a current efficiency of 75% (i.e. 5/6·7), consistent with the above work. The results of Jones and Peters [6], although mostly referring to very different conditions from those used here, provide two examples (7° C and 37° C in 0·1 M H_2SO_4 at 1·5 V) where comparisons can be made, and we calculate that the charges passed were 6·8 F and 6·7 F respectively, per mole of copper dissolved. There is thus wide agreement* on the stoichiometry of the anode reaction at ambient temperatures.

The anodic dissolution of chalcopyrite is in general a non-uniform process giving rise to pits and crevices in the electrode surface (see below). The properties of the sulphur product depended on the experimental conditions. At low potentials (1·0–1·1 V in 1 M H_2SO_4, 1·1–1·2 V in 1 M HCl) sulphur accumulated in the pits, was black in appearance and had a toffee-like consistency. Its insolubility in carbon disulphide suggests that it

* The conclusion reached by Zevgolis [3] that the process involved 4 F mol^{-1} seems, as has already been pointed out [6], to have arisen from a mathematical error in the interpretation of his original data which, according to our calculations, yield 8·1 or 10·9 F mol^{-1}, depending on the set of results used. These results no doubt contain a charge contribution from the cyclic reduction and re-oxidation of dissolved iron, since in the coulometric experiments anode and cathode were in the same compartment [3].

was an amorphous plastic form of sulphur. Bertram and Illi [5] also found the product to contain plastic sulphur. With standing over a period of days, the sulphur lightened in colour due to transformation to the yellow rhombic form. At higher potentials, yellow sulphur was the immediate product. With a rotating electrode in 1 M H_2SO_4 the sulphur formed at high potentials did not adhere to the surface which was left quite bright and etched so as to reveal the grains in the polycrystalline specimen.

Attempts were made to detect solid intermediate products with an electron microprobe (JEOL Model 50 JXA). An oxidized electrode (1 M H_2SO_4 1·01 V for 18 h, 71 C cm^{-2}) was sectioned and polished and the elemental composition determined at various points in the bulk and near the visible reaction interface. The composition appeared to change abruptly at the boundary between chalcopyrite and the product sulphur, with no indication of any copper or iron concentration gradient within the chalcopyrite. The lower limit of thickness of a metal-depleted layer detectable by this means would be of the order of the diameter of the electron beam (1 μm). Thus, layers thicker than this either do not form or are insufficiently stable (e.g. through re-equilibration with the bulk) to be retained until the probe measurement is made.

3.4. *Current–time behaviour*

Time-dependent currents with chalcopyrite anodes have already been noted by Jones and Peters [6]. The effects can be striking, with up to two orders of magnitude change in current at certain potentials (Fig. 4). We find a critical potential (~ 1·01 V in 1 M H_2SO_4, ~ 1·13 V in 1 M HCl) below which the current always decays with time and above which it passes through a minimum. This minimum is reached in shorter times as the potential is increased. In 1 M H_2SO_4 a second minimum may occur (Fig. 4). The origin of this current–time behaviour is discussed in the next section.

The steepness of the current–voltage relationship is emphasized if the current at longer time is considered, e.g. in Fig. 4b the current at 10 min increases by almost 3 decades between 1·13 V and 1·17 V. However, in the absence of a steady state it does not seem reasonable to construct polarization curves from such measurements for the purposes of determining kinetic parameters and a reaction mechanism.

3.5. *Surface morphology and nucleation phenomena*

As mentioned above, the anodic dissolution of chalcopyrite was not uniform over the surface. The

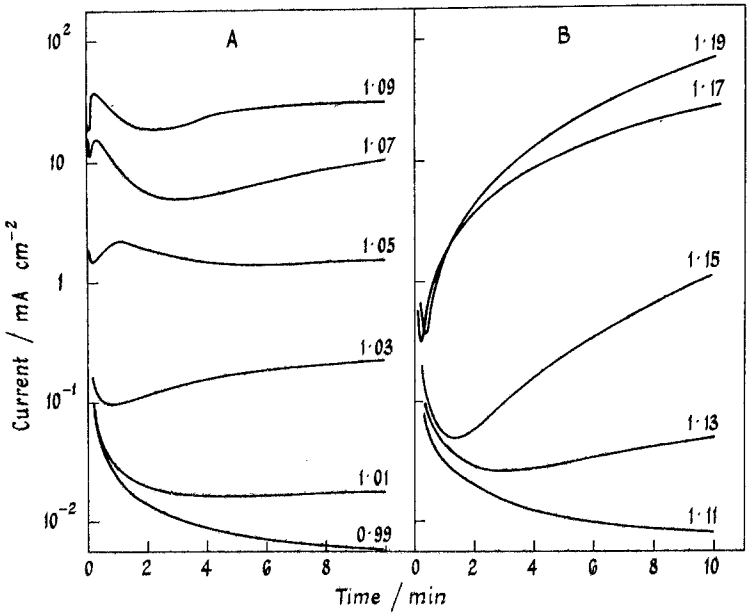

Fig. 4. Current–time curves at a stationary chalcopyrite electrode at the potentials indicated in (a) 1 M H_2SO_4, (b) 1 M HCl. Surface reground before each measurement.

extremes of this behaviour were seen at the lowest potentials at which significant current could be sustained. At 1·01 V in 1 M H_2SO_4, long periods (up to 3 days) of electrolysis left the bulk of the surface unattacked, with a thin region of deep corrosion at the edges of the specimen. Similarly, at 1·13 V in 1 M HCl, all of the reaction occurred at a few localized sites, though in this case they were distributed over the specimen.

As the potential was raised, the number of corrosion sites increased dramatically. Fig. 5 shows photographs of the electrode surface after passage

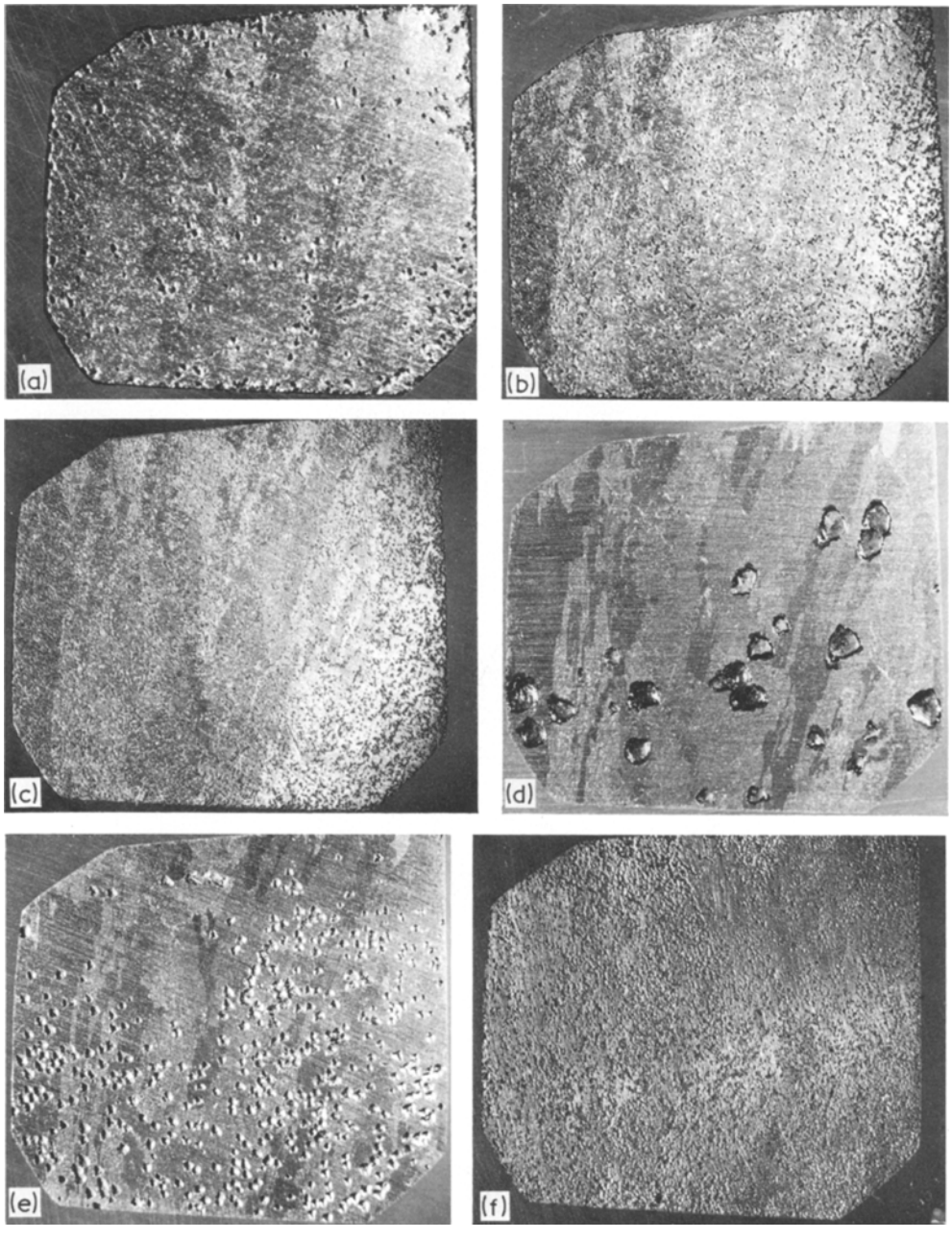

Fig. 5. Photographs of electrode (16 mm wide) after passage of 15 C cm^{-2} at the following potentials (in 1 M H_2SO_4): (a) 1·03 V, (b) 1·05 V, (c) 1·07 V. In 1 M HCl: (d) 1·13 V, (e) 1·15 V, (f) 1·19 V.

of a given amount of charge at various potentials. The pits in 1 M HCl were fairly regular in shape, while in 1 M H_2SO_4 they were elongated and distributed to form patterns on the surface, suggesting preferred nucleation along irregularities in the specimen and possibly along grain boundaries.

From photographs such as those in Fig. 5, counts were made of the density of corrosion pits as a function of potential and charge passed. The more regular shape made this an easier task in 1 M HCl, and the results for this electrolyte are plotted in Fig. 6; the behaviour in 1 M H_2SO_4 is qualitatively similar. Each point is from a separate experiment with a freshly ground surface. The number of pits (N) is seen to be an exponential function of potential and the slope $\partial E/\partial(\log N)$ is 15 mV. There is only a small dependence of N on charge passed (i.e. on time) at a fixed potential, with, if anything, a tendency for N to decrease, presumably due to amalgamation of adjacent pits.

The above results lead us to analyse the anodic behaviour of chalcopyrite according to well-established theories for electrode kinetics governed by the nucleation and growth of discrete reaction centres [11]. The lack of time-dependence of N suggests that the initiation of pits can be classed as an instantaneous nucleation process in which the number of corrosion nuclei is constant at a given potential. For hemispherical growth of pits, where the rate is proportional to the pit surface area, the current should increase with t^2, and indeed curves of the type shown in Fig. 4b do show substantial sections (about two decades of current) after the minimum where this relation is followed. The current then goes through a linear region and finally starts to level off. The picture is more complex in 1 M H_2SO_4 (Fig. 4a) but the presence of a second minimum in i/t curves is typical of the influence of overlap of discrete growth centres in a surface process [11].

Another phenomenon at least partly explained by the nucleation behaviour is the unusual hysteresis found in cyclic voltammograms at the foot of the main wave (Fig. 7). It appears that the upward trend of the current after reversal of the scan is due to the continued expansion of pits nucleated at the higher potential.

From the above evidence, we conclude that the kinetics of chalcopyrite dissolution in the steep part of the voltammogram are determined by the rate of nucleation and subsequent growth of ano-

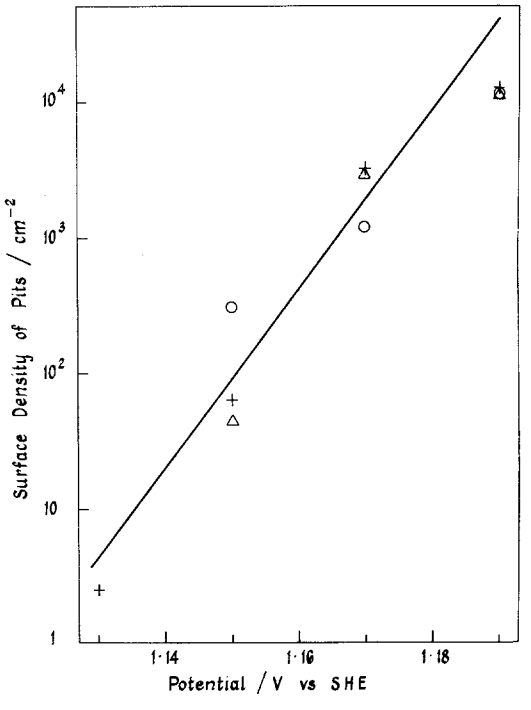

Fig. 6. Potential dependence of the density of corrosion pits on a ground chalcopyrite surface in 1 M HCl: ○, Moonta chalcopyrite, charge passed 17 C cm^{-2}; +, unknown origin, 5 C cm^{-2}; △, unknown origin, 11 C cm^{-2}.

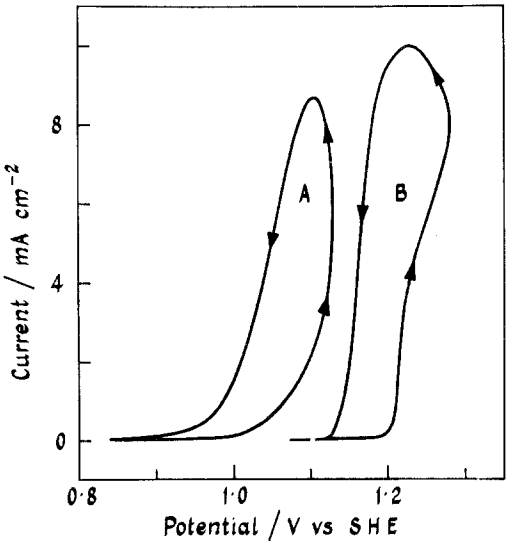

Fig. 7. Cyclic voltammograms (3rd cycle) at the foot of the main anodic wave (ground surface; 20 mV s^{-1}; rotation rate 50 rev s^{-1}). (a) 1 M H_2SO_4; (b) 1 M HCl.

dic reaction sites*. Current–time curves show an induction period during which the current decays but essentially all the sites nucleate, an intermediate period of three-dimensional growth of pits, and a period when the dissolution rate begins to be influenced by the overlap of pits and, probably, by the accumulation of sulphur. The number of nuclei depends strongly on potential and this seems to underly the steepness of the current–voltage curve.

The localized dissolution of chalcopyrite is analogous to the pitting corrosion of metals where breakdown of a passive film occurs when a critical potential is reached (see e.g. [13]). It is tempting to suggest that the passive film in the case of chalcopyrite is the postulated metal-deficient prewave product layer and that this breaks down at the critical potential when the reaction to give sulphur is initiated. The main argument against this idea is that elemental sulphur can be formed, at least under conditions of ferric leaching, at much lower potentials, and, as such leaching can display parabolic kinetics [9, 10], the reaction is presumably uniform over the surface. Thus, although the continued oxidation of chalcopyrite may not necessarily involve pitting, we suggest, for the reasons given below, that pit formation is a prerequisite to *high* dissolution rates.

Explaining the kinetics of the ferric leaching of chalcopyrite is a central problem, made more difficult by conflicting reports of the form of the rate equation, with both linear and parabolic kinetics being found (see [14] for a review). The most common explanation for parabolic kinetics involves inhibition of the diffusion of reactants by a thickening porous film of sulphur. Linge [9] has rejected this on the grounds that the measured rate constants are too small and that a pore diffusion mechanism cannot account for observed activation energies and reactant concentration effects. He introduces a model [9] in which the initially formed metal-deficient layer remains beneath the sulphur during the oxidation process, and solid-state diffusion through that layer is rate-determining.

Our own results add little to the controversy except to suggest that the physical properties of plastic sulphur may allow it to form a sufficiently dense layer to give the observed low rates of leaching. Certainly, we see no grounds for taking the theoretical volume decrease according to Reaction 2 (25–34% depending on the type of sulphur) as the basis for calculating porosity. An additional point is that a pore diffusion mechanism will give rates which are very sensitive to changes in the physical form of the sulphur layer and it is therefore possible that slow, temperature-dependent recrystallization processes in the sulphur could explain the observed activation energies and even the discrepancies between results of different studies.

The view that the slowness of the leaching reaction is due to a passivating sulphur film requires that this film forms a more or less uniform compact layer. Any acceleration of the reaction (such as occurs at high potentials) would require either a change in the properties of the sulphur or some type of non-uniform distribution which leads to localized thinning of the layer or exposure to fresh surface. We suggest that pits act in the latter way, with plastic sulphur accumulating, through surface forces, at the bottom of a pit and the reaction thereby occurring more rapidly at the walls. Since we have also observed that the physical properties of the sulphur formed depend on potential and type of electrolyte, these may also be possible factors controlling pit initiation or the kinetics of oxidation at high potentials.

3.6. *The high potential region: illumination effects*

Here we consider the voltammogram at potentials positive to the very steep section. The high potential limit used in these studies, nominally 5·25 V, was chosen because of the interest in Zevgolis' observations [3, 4] at such high apparent potentials. However, substantial corrections to these values are required with resistive electrodes (typically 1–5 Ω in our work) at high current densities, and the potential values should be regarded as nominal. Linearity of the voltammogram before

*A very different process involving chalcopyrite, the initial reduction of a thin surface layer prior to bulk reduction to chalcocite, has also been analysed in terms of the expansion and overlap of growth centres [12]. Progressive nucleation was favoured in that work, but the kinetics would also be consistent with an instantaneous nucleation process in which $\partial E/\partial(\log N) = -17$ mV (the negative value refers to a cathodic reaction). The similarity in absolute values of the slopes is noteworthy, though we are reluctant to assign any basic significance to this.

the current peak (Fig. 2) indicates resistive control in this region.

In 1 M H_2SO_4 (Fig. 2) there is a maximum and then a decline in current, on positive-going scans. The behaviour in 1 M HCl cannot be so simply described because of continuous changes with cycling, but in general there were one or two plateau regions between 1·3 and 2·5 V followed by a rise in current to the potential limit. In both electrolytes the current levels were a good deal higher than reported by Zevgolis [3, 4] although in those studies a mixed electrolyte (1·53 M H_2SO_4, 0·856 M NaCl) was employed. The plateaux in 1 M HCl occurred in the range 0·3–0·5 A cm^{-2}, about 10 times greater than the plateau reported in [3], and the maximum current reached was 2·6 A cm^{-2}, also larger by a factor of 10. In 1 M H_2SO_4 the peak current we observed was 1·1 A cm^{-2} at a sweep rate of 200 mV s^{-1}; lower values were obtained at slower scanning rates. This suggests that the potentiodynamic method of measurement probably accounts in part for the higher currents found here, but other unidentified factors seem to be involved.

In view of the results of Zevgolis [3, 4] we undertook a search for photoeffects in the high potential region. The white light source was a Schott model KL150 which uses a 150 W halogen lamp to produce a narrow, high-intensity beam from a fibre optic light conductor. The beam was directed at the electrode surface from below the glass cell and the light path therefore included 4 cm of electrolyte. Photoeffects were sought by comparing complete voltammograms in the dark and with illumination (a valid method in 1 M H_2SO_4 where successive sweeps gave reproducible voltammograms), and by a crude type of modulation where the light source was switched on and off at short intervals. In neither case did the light have any effect on the recorded current.

Thus, although chalcopyrite is an n-type semiconductor [15] it does not display a photosensitive anodic limiting current characteristic of rate-determining diffusion of minority carriers. We therefore cannot agree with the earlier conclusion [3, 4] that the anodic behaviour of chalcopyrite is determined by its semiconducting properties. Certain unsatisfactory features of the work quoted [3, 4] have already been pointed out [16] but do no entirely explain the discrepancy in experimental results. Particular criticism can be levelled at illumination of the rear rather than the working surface of the electrode, since charge recombination would eliminate any increase in hole concentration at distances of the order of 1 cm from the illuminated surface.

Beyond allowing the conclusion that semiconductor behaviour plays no part, the present evidence is inadequate for a detailed explanation of voltammogram shapes at high potentials. The influence of a thick sulphur layer on the electrode kinetics is probably important, and the evolution of oxygen or chlorine as side reactions may play a part.

3.7. *Reactivity comparisons*

3.7.1. Electrolyte effects. Chalcopyrite is anodically more reactive in 1 M H_2SO_4 than in 1 M HCl (Fig. 7). This may seem a surprising result in view of the well-known greater leaching activity of ferric chloride solutions compared with ferric sulphate [17] but is consistent with the finding that chalcopyrite leached more slowly when chloride was added to a ferric sulphate medium, so long as the temperature was 40° C or less [18]. The practical advantages of a ferric chloride leachant probably reside in factors such as solubility and complexing properties [17] rather than in any intrinsically 'aggressive' nature of the chloride ion in this system.

3.7.2. Influence of mineral origin. Reactivities of four chalcopyrite specimens* were compared under the conditions of Fig. 7. In each of the two electrolytes, voltammograms were similar in shape and in actual levels of current. For example, at 1·13 V in 1 M H_2SO_4 (first positive-going scan with a freshly ground surface) currents ranged from 15–24 mA cm^{-2} on the four electrodes. The behaviour was also similar in the high potential region, although the different internal resistances of the electrode produced differences in the position of the peak in 1 M H_2SO_4. For the samples studied, therefore, the source of the mineral has little effect on the rate of chalcopyrite dissolution, at least in the potential region of significant anodic current.

*Moonta (South Australia), Mt. Lyell (Tasmania), Ookiep Mine (South Africa) and synthetic.

There is a special interest in the relationship between mineral origin and reactivity of sulphide minerals, because their semiconducting nature provides an easily accessible set of properties which can differ markedly from sample to sample [15], generally due to the influence of impurities. The present results, showing only small variations for chalcopyrite, are similar to the findings for the oxygen reduction reaction on pyrite electrodes [16] where reactivities differed much less than might be expected from differences in electrical properties. On the other hand, there is evidence from leaching studies [19] that the reactivities of different chalcopyrite specimens (as constituents of impure concentrates) can very significantly, though not necessarily due to semiconductor effects. One must be cautious in comparing electrolysis with leaching results because of the very different potentials (probably 0·5 V) and time scales involved, and it cannot yet be decided whether these data are really in conflict.

4. *Conclusions*

The following conclusions were reached:

(a) For the bulk anodic dissolution of chalcopyrite electrodes in 1 M H_2SO_4 or 1 M HCl at 25° C, the charge involved is 6·7 ± 0·3 F per mole and the mole ratio of sulphur to sulphate produced is about six. Some of the product is plastic sulphur. No intermediate solid products are detectable on the electrode surface.

(b) At potentials below the region of active dissolution there is a voltammetric prewave which represents a surface oxidation process consuming a charge of around 1 mC cm^{-2}. There is evidence to suggest that the surface reaction involves the selective dissolution of iron.

(c) The reaction rate in the steep region of the current–voltage curve is determined by the kinetics of nucleation and three-dimensional growth of anodic dissolution sites. The steepness of the curve is related to the strong dependence of the rate of nucleus formation on potential, with a tenfold increase over 15 mV. Current–time behaviour is also characteristic of the expansion and overlap of localized dissolution centres.

(d) At high potentials, where plateaux or maxima can be found in the voltammograms, the current is not influenced by illumination and there is no indication that the semiconducting nature of chalcopyrite determines its anodic behaviour.

(e) No pronounced influence of the chalcopyrite specimen origin on current–voltage behaviour is detectable.

References

[1] K. N. Subramanian and P. H. Jennings, *Canad. Metall. Quart.* **11** (1972) 387.
[2] G. Springer, *Inst. Mining Met. Trans. Sect. C* **79** (1970) 11.
[3] E. N. Zevgolis, Ph.D. Thesis, University of Minnesota (1971).
[4] E. N. Zevgolis and S. R. B. Cooke, *Proceedings Eleventh International Mineral Processing Congress*, Cagliari, Universita di Cagliari (1975) p. 449.
[5] R. Bertram and H. Illi, *Chem.-Ing.-Tech.* **48** (1976) 141.
[6] D. L. Jones and E. Peters, 'High Temperature High Pressure Electrochemistry in Aqueous Solutions', NACE-4, National Association of Corrosion Engineers, Houston (1976) p. 443.
[7] T. Biegler, D. A. J. Rand and R. Woods, *J. Electroanalyt. Chem.* **60** (1975) 151.
[8] T. Biegler and D. A. Swift, *J. Appl. Electrochem.* **6** (1976) 229.
[9] H. G. Linge, *Hydrometallurgy* **2** (1976) 51.
[10] J. P. Baur, H. L. Gibbs and M. E. Wadsworth, 'Initial stage sulfuric acid leaching kinetics of chalcopyrite using radiochemical techniques', Paper 72-B-96 at *Annual AIME Meeting*, San Francisco (1972).
[11] M. Fleischmann and H. R. Thirsk, 'Advances in Electrochemistry and Electrochemical Engineering' (Ed. P. Delahay), Vol. 3, Interscience, New York (1963) Ch. 3.
[12] T. Biegler, *J. Electroanalyt. Chem.* **85** (1977) 101.
[13] H. H. Uhlig, 'Corrosion and corrosion control' (2nd ed.), John Wiley, New York (1971) Ch. 5.
[14] J. E. Dutrizac and R. J. C. MacDonald, *Minerals Sci. Eng.* **6** (1974) 59.
[15] R. T. Shuey, 'Semiconducting ore minerals', Elsevier, Amsterdam (1975).
[16] T. Biegler, *J. Electroanalyt. Chem.* **70** (1976) 265.
[17] R. J. Roman and B. R. Benner, *Minerals Sci. Eng.* **5** (1973) 3.
[18] J. E. Dutrizac and R. J. C. MacDonald, *Met. Trans.* **2** (1971) 2310.
[19] H. G. Linge, *Hydrometallurgy* **2** (1976/1977) 219.